Review Article

http://dx.doi.org/10.3348/kjr.2011.12.6.651
pISSN 1229-6929 · eISSN 2005-8330
Korean J Radiol 2011;12(6):651-661

Korean Journal of Radiology
KJR

Diffusion Tensor Imaging: Exploring the Motor Networks and Clinical Applications

Sungsoo Ahn, MD, Seung-Koo Lee, MD

All authors: Department of Radiology, Yonsei University College of Medicine, Seoul 120-752, Korea

With the advances in diffusion magnetic resonance (MR) imaging techniques, diffusion tensor imaging (DTI) has been applied to a number of neurological conditions because DTI can demonstrate microstructures of the brain that are not assessable with conventional MR imaging. Tractography based on DTI offers gross visualization of the white matter fiber architecture in the human brain *in vivo*. Degradation of restrictive barriers and disruption of the cytoarchitecture result in changes in the diffusion of water molecules in various pathological conditions, and these conditions can also be assessed with DTI. Yet many factors may influence the ability to apply DTI clinically, so these techniques have to be used with a cautious hand.

Index terms: *Diffusion tensor imaging; Tractography; Diffusion weighted imaging*

INTRODUCTION

Ever since diffusion weighted imaging (DWI) was introduced in 1986 by Le Bihan et al. (1), diffusion magnetic resonance (MR) imaging techniques have rapidly advanced and especially for the evaluation of the central nervous system. Among them, diffusion tensor imaging (DTI) reveals diffusion anisotropy and the directional distribution of water diffusivity and so it enables physicians/scientists to investigate microstructures and to map the white matter fiber tracts in the human brain *in vivo*, which is impossible with conventional MR imaging. Regardless of some limitations, the development of imaging and the post-processing techniques has contributed to the widespread use of DTI for various neurological conditions (2-8).

In this paper, we will briefly review the principles and techniques of DTI as well as its limitations. Exploring the white matter anatomy by DTI, the practical application of tractography in neurosurgical and neurological diseases and other general considerations will also be discussed.

Received March 29, 2011; accepted after revision June 3, 2011.
This study was supported by a grant from the Korea Research Institute of Bioscience & Biotechnology (KRIBB) Research Initiative Program.

Corresponding author: Seung-Koo Lee, MD, Department of Radiology, Yonsei University College of Medicine, 50 Yonsei-ro, Seodaemun-gu, Seoul 120-752, Korea.
• Tel: (822) 2228-2373 • Fax: (822) 393-3035
• E-mail: slee@yuhs.ac

Basic Principles

When water molecules diffuse equally in all directions with no preferential direction, the diffusion is considered to be isotropic. On the other hand, diffusion of free water in the body is not always the same in all directions of three-dimensional (3D) space, which is defined as anisotropic diffusion. For example, in contrast to cerebrospinal fluid (CSF) where diffusion of water molecules is random and isotropic, diffusion anisotropy is often caused by the orientation of fiber tracts in the white matter as water diffuses in a direction parallel to the axon's longitudinal axis due to the axonal fibers and their myelin sheaths (9).

Diffusion anisotropy represents the amount of

directionality and this is affected by the physiochemical properties of the tissue and its micro-/macrostructures (10). The differences in the diffusivity of water molecules can be measured by applying a pair of strong gradients, which is known as diffusion weighting. The degree of diffusion weighting is defined by the b value and this is determined by the type of sensitizing gradient scheme. DWI is usually obtained with a b value ranging from 700 to 1200 sec/mm^2 and a b value of 0 sec/mm^2 (the b0 image) (11-13).

Diffusion tensor was developed to characterize the diffusion in anisotropic voxels and it describes the properties of a diffusion ellipsoid in 3D spaces. It has 3 eigenvalues ($\lambda_1 \geq \lambda_2 \geq \lambda_3$), which represent the magnitude of the diffusivities, and 3 eigenvectors (v_1, v_2, v_3), which signify the direction of diffusion within a voxel and these 3 eigenvectors are orthogonal to one another (Fig. 1). The diffusivity along the principal axis, which is the direction of the maximum diffusion, is λ_1 and the 2 small axes are λ_2 and λ_3. Six elements of the diffusion coefficient (Dxx, Dyy, Dzz, Dxy, Dxz, and Dyz) for each voxel are calculated from six images that are obtained by applying diffusion weighted gradients in at least 6 directions in order to measure the diffusion properties of water in 3D space and then the 3 eigenvalues and 3 eigenvectors can also be obtained from these elements. The quantity and directionality of the anisotropic diffusion in the white matter can be demonstrated on various maps (i.e., fractional anisotropy map, color-coded map, fiber tractography), and these will be discussed below.

Data Acquisition

Diffusion tensor imaging can be obtained by using a b value of 0 sec/mm^2 and diffusion weighted gradients in at least six orientations, as was mentioned before. While Hasan et al. (13) reported that there is no significant advantage to using more than six encoding directions as long as an optimum encoding is used for the six directions, Jones et al. (14) showed that at least 20 unique sampling orientations for anisotropy or 30 for tensor-orientation and the mean diffusivity are required for a robust estimation unless time is limited.

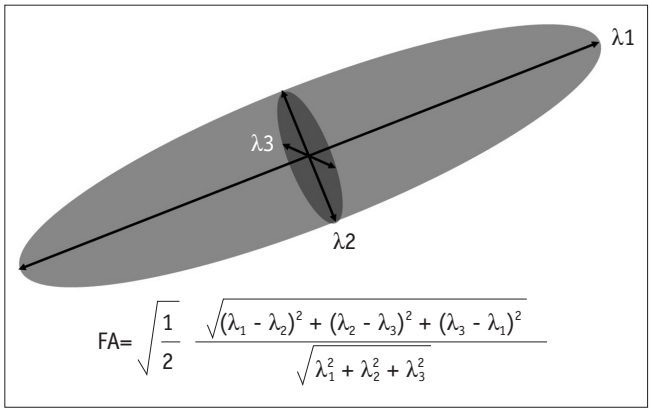

Fig. 1. Calculation of fractional anisotropy. Largest vector of diffusion ellipsoid is eigenvector 1 and its value is λ1. Shortest one is λ3 and remainder is λ2. Fractional anisotropy is calculated by each of eigenvalues. Fractional anisotropy varies from 0 (infinite isotropy) to 1 (infinite anisotropy).

Fast acquisition techniques such as echo-planar imaging (EPI) are generally used for DTI since motion-related artifacts may induce misinterpretation of diffusivity (15). Although multishot EPI has an advantage over single-shot EPI in terms of the greater spatial resolution, the greater signal-to noise ratio and less susceptibility-related distortion, the use of multishot EPI is limited due to its longer data acquisition time. Therefore, cardiac gating, CSF suppression and navigator echo correction have been implemented to reduce motion-related artifacts, which also prolong the imaging time (16-18). Single-shot EPI with acquiring the entire set of echoes within the same motion-induced error is commonly used in practice with a shorten image acquisition time to less than 5 min and sufficient tractographic results (19). For the EPI, the reduction of phase-encoding steps with a parallel imaging technique will lead to a reduction in the readout length for data acquisition, and this may result in a major reduction in image distortion. In addition, with the advances in 3.0-Tesla (T) MRI, a higher signal-to-noise ratio of the images can be obtained. A previous study compared the depiction of fiber tracts at 3.0- versus 1.5-T DT tractography with parallel imaging and that study revealed better visualization of fiber tracts at 3.0T (20). In addition, high-spatial-resolution DTI of the brainstem, where image distortion can be especially troublesome with conventional EPI, has been achieved at 3.0T with parallel imaging (21).

Techniques

Fractional anisotropy (FA) is a measure of anisotropic water diffusion, which is the shape of diffusion with a scalar value (22). FA is computed by comparing each eigenvalue with the mean of all the eigenvalues (mean diffusivity [MD]: $<\lambda>$). FA ranges between 0 and 1, where 0 means isotropic diffusion and 1 indicates infinite anisotropic diffusion. The FA map, as demonstrated with FA values, describes the degree of diffusion anisotropy in each voxel, and so this reflects the degree of directionality of cellular structures

Korean Journal of Radiology
KJR

within the fiber tracts. For example, white matter, where anisotropy is high, shows the bright end of the gray scale, whereas gray matter reveals the dark end of the gray scale (Fig. 2). Similarly, a loss of anisotropic diffusion can be related to abnormalities within the cellular microstructure.

A color-coded map may be a more practical way of visualizing the data as it can be generated from eigenvalues and eigenvectors, of which the intensities are scaled in proportion to the FA and the elements are conventionally assigned to red (x element, left-right), green (y, anterior-posterior) and blue (z, superior-inferior) (23). For example, the corpus callosum that runs along the transverse axis is assigned to red, while the corticospinal tract that runs along the superior-inferior axis is assigned to blue.

The tensors of cerebral white matter can be reconstructed to track the 3-D fiber orientation from voxel to voxel and so the fiber tractography (FT) can demonstrate the gross fiber architecture by assuming that the direction of the least restricted diffusion represents the orientation of the nerve fibers. One method that is commonly used for FT is line propagation or the streamline techniques (24). When we set one or multiple regions of interests (ROIs) in the course of fiber projections in relation to known anatomic landmark, the tracking starts from a voxel from which a line is propagated in both the retrograde and antegrade directions based on the principle axis. Therefore, basic knowledge of brain anatomy is a requisite for drawing the starting and target lesions. Tracking is terminated when the fiber tract encounters a voxel with FA below the threshold value, and usually between 0.1 and 0.2, or a trajectory angle larger than the threshold, and usually between 25 and 45 degrees, by which in the vivo FT can be generated (Fig. 3).

Probabilistic tractography is another way to reconstruct fiber trajectories (25, 26). In contrast to the streamline approach that can reconstruct only one trajectory per seed voxel, the probabilistic approach is able to depict multiple pathways arising from the seed voxel by computing the probability of the dominant streamline passing through any single region (Fig. 4). Therefore, this technique enables quantitatively evaluating the potential connectivities between the regions that have not been able to be identified on FT because of their nondominancy or uncertainty.

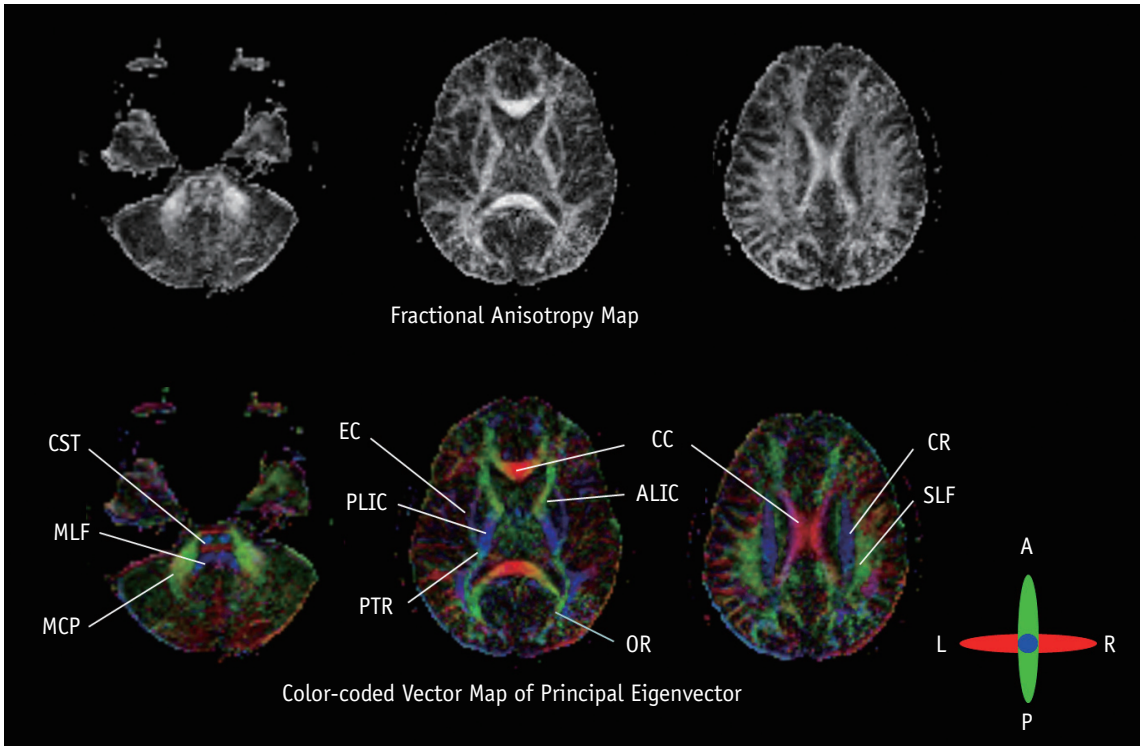

Fig. 2. Gray and color scale fractional anisotropy maps. High signal on fractional anisotropy map indicates higher anisotropy such as corpus callosum and internal capsule. On color scale fractional anisotropy map, red fibers represent transverse direction, green represents anterior to posterior direction and blue represents head to foot direction. ALIC = anterior limb of internal capsule, CC = corpus callosum, CR = corona radiata, CST = corticospinal tract, EC = external capsule, MCP = middle cerebellar peduncle, MLF = medial longitudinal fasciculus, OR = optic radiation, PLIC = posterior limb of internal capsule, PTR = posterior thalamic radiation, SLF = superior longitudinal fasciculus.

Clinical Applications

Exploring Normal White Matter Tracts: Motor Network

As the diffusion in white matter is strongly anisotropic, DTI and FT can be used to demonstrate the white matter architecture and reconstruct the 3-D neuronal pathways. Some studies have tried to construct white matter atlases using DTI so that we can better understand white matter structures and their abnormalities (2, 27). Among the white matter tracts, it is important to be aware of motor networks as motor dysfunction correlates well with the location and extent of the involved motor cortex and the various white matter tracts associated with voluntary or involuntary movement. For example, as the corticospinal tract at the level of the internal capsule is known to be organized somatotopically, the lesion location correlates well with the patient's symptoms (28). The detailed anatomy of the corticospinal tract can be depicted with DTI-FT by placing ROIs in the longitudinal pontine fibers, the posterior limb of the internal capsule and the primary and premotor areas of the cerebral cortex (Fig. 5). Further, a color-coded map demonstrates four major fiber bundles in the centrum semiovale, where the conventional MR image shows homogeneous signal intensity, so that we can identify the corona radiate with including the corticospinal tract, the corticobulbar tract and the corticopontine tract (Fig. 6).

The motor cortex is connected with other cortical areas and not only with adjacent gyri, but also with widely spaced gyri (29, 30). The arcuate fasciculus, which is also seen as a part of the superior longitudinal fasciculus, runs from the pars triangularis and opercularis of the inferior frontal gyrus (Broca's area) into the superior temporal gyrus and inferior parietal lobule (Wernicke's area) and the arcuate fasciculus is also well demonstrated. Interestingly, this pathway shows strong asymmetry in the relative fiber density and FA and it is usually dominant on the left side (Fig. 7). This finding is consistent with the left lateralization of language function in most humans.

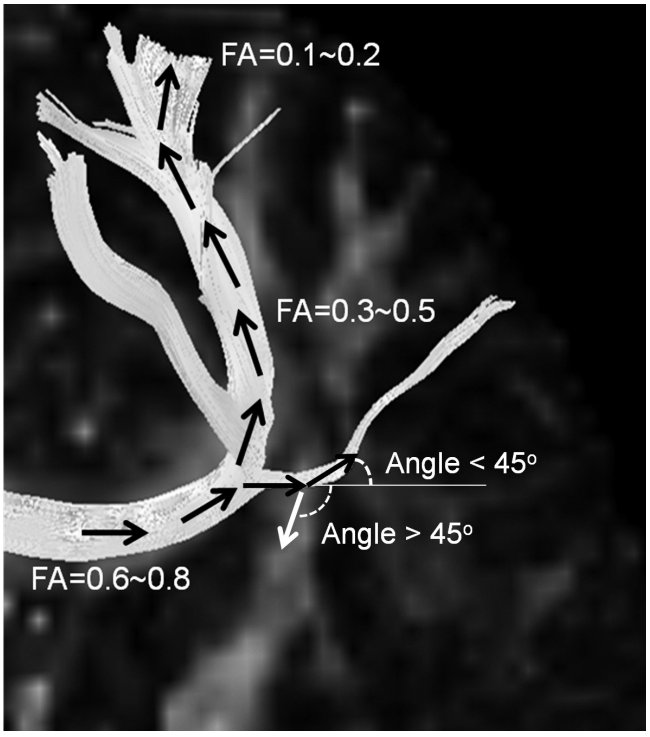

Fig. 3. Principle of streamline fiber tracking. From starting point, automatic 3-D fiber tracking is done by connecting voxel to voxel with pre-defined threshold values of fractional anisotropy (FA) and trajectory angle. Fiber tracking terminates when fractional anisotropy is lower and trajectory angle exceeds threshold values. For clinical fiber tracking, fractional anisotropy of 0.1-0.2 and trajectory angle of 30-45 degrees are usually used.

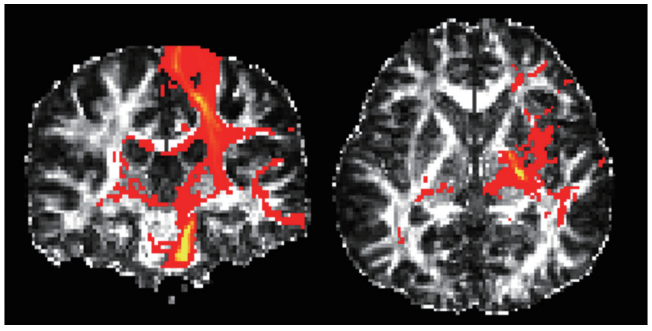

Fig. 4. Probabilistic map of left corticospinal tract. Yellow area has higher probability of connection such as longitudinal pontine fibers and corticospinal tract that innervates the lower extremities. There can be some connectivity to ipsilateral temporal lobe, contralateral hemisphere or basal ganglia, although probability is very low. Overall shape is similar to streamline tractography in next figure.

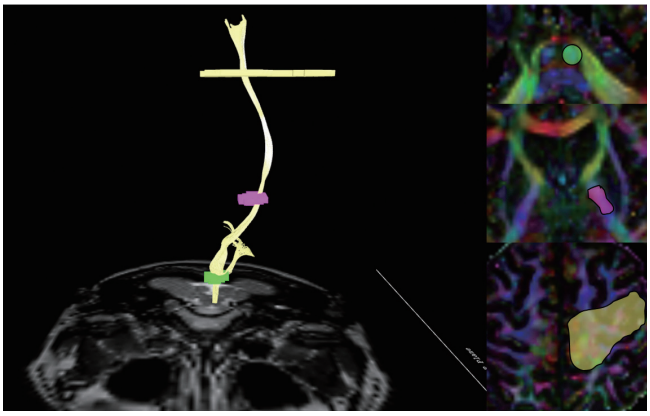

Fig. 5. Streamline tractography of corticospinal tract. Three regions of interests are placed at longitudinal pontine fibers, mid-1/3 of posterior limb of internal capsule and primary sensory-motor cortex. These anatomic landmarks are preferred because they are easily localized and they are reliable pathways of corticospinal tract.

Korean Journal of Radiology
KJR

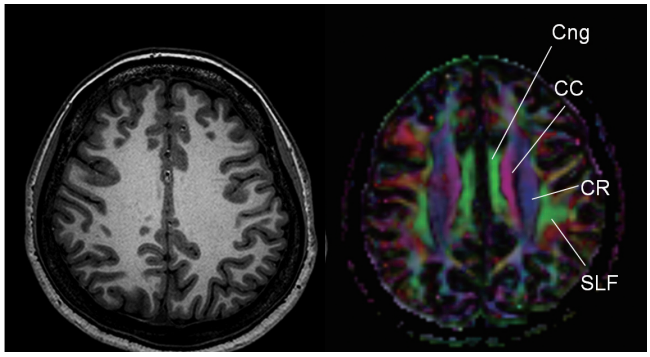

Fig. 6. Diffusion tensor imaging shows 4 different tracts intermingled in centrum semiovale. Cingular fibers (Cng) runs antero-posteriorly. CC = corpus callosum, CR = corona radiata, SLF = superior longitudinal fasciculus

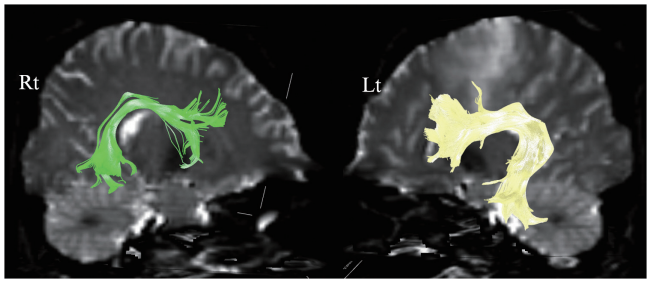

Fig. 7. Arcuate fasciculus (superior longitudinal fasciculus) connecting Broca's area and Wernicke's area. Right-left asymmetry is reported and usually dominant hemisphere has larger volume of arcuate fasciculus.

The basal ganglia constitute a major structure for the operation of the entire motor system. Although some of the fibers associated with motor function between the thalamus and the basal ganglia cannot be demonstrated on FT due to other fibers crossing this area, the basal ganglia have connections with a large part of the cerebral cortex on FT, which suggests that the basal ganglia are the hub of motor connections.

The cerebellum is an important component of the motor system and it contributes to coordination. The superior cerebellar peduncle is the major output pathway of the cerebellum and the dentato-rubro-thalamo-cortical connection is a major pathway that passes through this peduncle, and the dentato-rubro-thalamo-cortical connection may be reconstructed with FT by locating ROIs in the primary and premotor areas, the thalamus, the red nucleus and the superior cerebellar peduncle (Fig. 8).

The middle cerebellar peduncle is entirely composed of more than 20 million afferent fibers originating from the sensory and motor areas of the opposite cerebral cortex via the pontine nuclei and these fibers form the largest fiber system in the brain. Fiber tracts of the middle cerebellar

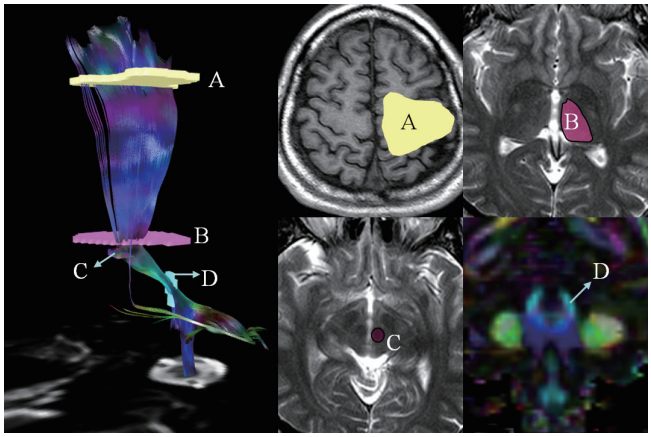

Fig. 8. Dentato-rubro-thalamo-cortical connection, which is major ascending fiber system from cerebellum to cerebral cortex. Region of interests are placed in each of anatomic locations (A = primary and premotor, B = thalamus, C = red nucleus, D = superior cerebellar peduncle).

peduncle form the transverse pontine fibers and some extend the cortical connections superiorly.

By demonstrating the motor networks with DTI-FT, we may be able to understand the clinical manifestations that are particularly associated with the white matter abnormalities that occur in developmental, neoplastic, demyelinating and neurodegenerative disorders, as well as helping to predict the motor sequelae preoperatively.

Pre-Surgical Planning

Diffusion tensor imaging-FT is beneficial for the surgical planning as well as for the postoperative assessment. With co-registration of DTI-FT to the high resolution anatomic images, we can use these techniques for surgical navigation (3).

Defining the relationship between brain tumors or vascular malformations and the eloquent cortices and pathways, such as the motor, sensory and language tracts, is crucial for determining the extent of resection to minimize any postoperative neurologic deficits (Fig. 9). The most common target for this evaluation is the corticospinal tract, which is the most direct pathway from the cerebral cortex to spinal motor neurons. Laundre et al. (31) reported that the preoperative corticospinal tract involvement determined on DTI was predictive of the presence of motor deficits, and even when the motor cortex was not involved. In addition, FT can be used to assess the reorganization of white matter after surgical resection of brain lesions, which was reported to be well correlated with neurological functions (32). However, a disrupted tract does not necessarily represent

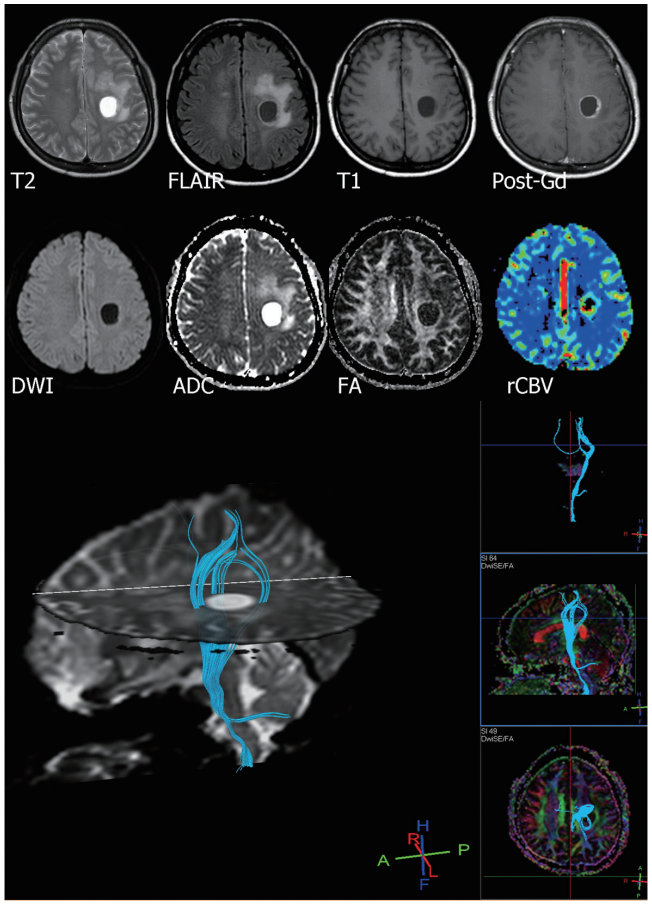

Fig. 9. 28-year-old female with anaplastic astrocytoma. Tractography clearly visualizes that mass is located at center of corticospinal tract.

direct damage to the tract, but this can be commonly noted to be a result of vasogenic edema and tract compression by the mass. Therefore, these techniques have to be used with a measure of caution.

Another issue for surgical planning is to delineate the exact margins of tumor infiltration as both tumor infiltration and peritumoral edema show T2 hyperintensity. The previous reports suggested that the MD and FA obtained from DTI may be helpful to distinguish tumor infiltration from vasogenic edema composed purely of extracellular water and consequently, to determine a tumor's resectability and the surgical approach (33, 34).

In addition, DTI-FT can be used for the surgical planning of not only tumors, but also for epilepsy. DTI-FT is helpful to determine whether seizure foci involve the eloquent areas such as optic radiations as well as to assess the completeness of disconnection following callosotomy in patients with intractable epilepsy even after a period of years (4, 35, 36) (Fig. 10).

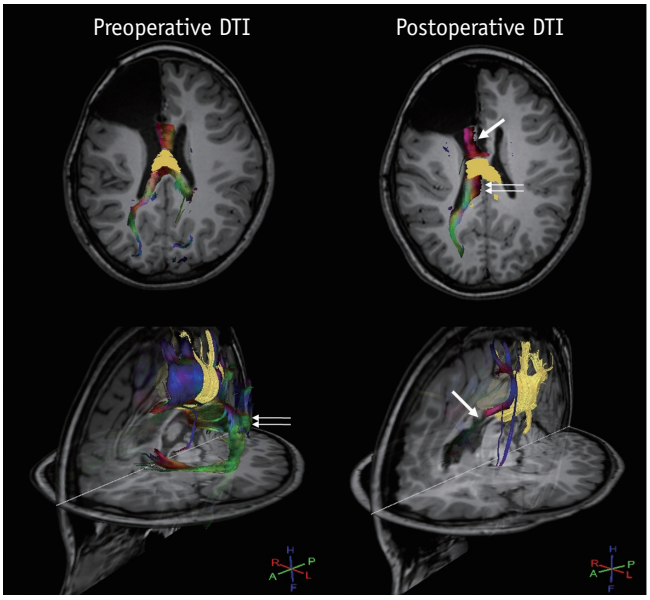

Fig. 10. 14-year-old male with intractable seizure and previous right frontal lobectomy status. Selective callosotomy was planned because patient complained of repeated seizure attacks. Yellow fibers indicate commissural fibers between bilateral sensory-motor cortex, which were preserved after callosotomy, while other callosal fibers were disconnected (thick arrow at frontal fibers and thin arrows at splenial fibers).

Ischemic Stroke

Acute cerebral ischemia results in cytotoxic edema and a decrease in the extracellular volume fraction, and consequently this restricts diffusion in the ischemic brain (37, 38). We can measure the tissue water diffusion with the MD of DTI, which removes the effects of anisotropy and myelin fiber orientation. Previous studies of both experimental and human stroke have demonstrated that the MD decreased in the acute phase was followed by normalization several days after stroke and there was a subsequent increase in the chronic phase (5, 39). On the other hand, the diffusion anisotropy was elevated acutely and subacutely, but then it began to decline and it remained reduced in chronic infarcts. Therefore, the investigators identified three phases of diffusion abnormality (5): 1) reduced MD and elevated anisotropy, 2) reduced MD and reduced anisotropy and 3) elevated MD and reduced anisotropy. During the subacute and chronic phases of ischemia, degradation of restrictive barriers allows a larger net displacement of the water molecules and the result is an increased MD, whereas disruption of the cytoarchitecture results in a significant reduction in diffusion anisotropy.

We can also predict clinical sequelae with FT by assessing the relationship between the eloquent fiber tracts and

Korean Journal of Radiology
KJR

small brain infarcts. For example, in patients with anterior choroidal artery infarcts, which involve the corticospinal tract and they cause motor dysfunction, reduced FA in the affected site and fiber disruption of the corticospinal tract may be an indicator of an unfavorable outcome (40). In addition, precise topographical evaluation with FT enables specific localization of lacunar infarctions in the corticospinal tract with regard to the affected body parts (28).

Similarly, the number of arcuate fasciculus fibers can be used to predict the prognosis of aphasia in patients with left middle cerebral artery infarcts, and this is of great clinical benefit (41). As mentioned above, the arcuate fasciculus normally shows asymmetry on FT, yet the patients with aphasia due to left middle cerebral artery infarcts lose the leftward asymmetry of these fibers, which may be a potential predictor of persistent aphasia.

In patients with stroke, measuring the changes of anisotropy with DTI may be useful for characterizing the progression of the ischemic lesion as well as assessing the potential outcome in response to the initial ischemic injury (Fig. 11).

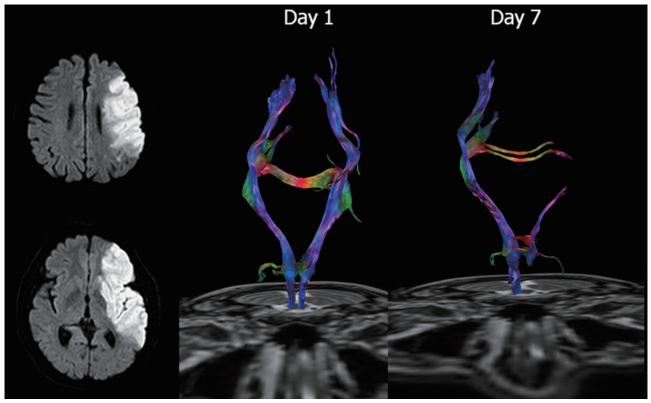

Fig. 11. 60-year-old male with left middle cerebral artery infarct. Initial diffusion weighted MRI shows acute infarct affecting left middle cerebral artery territory, including left corona radiate at level of centrum semiovale. Internal capsule at basal ganglia level is not affected. Initial tractography shows intact corticospinal tract, yet follow up scan 7 days after stroke reveals early injury to corticospinal tract, i.e., early start of Wallerian degeneration after major infarct.

Developmental Anomaly

Diffusion tensor imaging has been used for the non-invasive evaluation of cortical development in preterm newborns and for detecting derangement of its cytoarchitecture. High anisotropy of the cortex in the developing brain reflects the radial glial fiber system that guides the neuronal migration from the ependymal portion to the cortex (42). DTI also provides a better understanding of the pathogenetic mechanisms of developmental anomalies by describing the fiber pathways and aberrant fiber connections. Although DTI has limited values for evaluating the gray matter abnormalities due to the low FA of the gray matter, the white matter adjacent to the dysplastic cortex can be assessed by DTI-FT. In cortical dysplasia, decreased FA around the corticomedullary junction and decreased fiber connections around the affected area in comparison with the normal contralateral side have been demonstrated (6). When combined with other imaging modalities such as MR spectroscopy and advanced sequences like double inversion recovery and positron emission tomography (PET), DTI provides additional information for making the definite diagnosis of cortical dysplasia (Fig. 12). In patients with band heterotopias, a previous study suggested that the areas of high connectivity found in the band heterotopias in accordance with the histopathologic findings and the absence of focal neurologic deficit indicated the structural basis of the functional connectivity (43). Although complete or partial agenesis of the corpus callosum can be readily diagnosed on conventional MR imaging, DTI-FT provides additional information about the fibers connected through a partially remaining corpus callosum (6). Hoon et al. (44) reported that the disruption of sensory connections is responsible for motor impairment in patients with periventricular leukomalacia. On DTI-FT, the connecting fibers connected to the sensory cortex were markedly reduced, whereas the corticospinal tracts appeared normal.

Neurodegenerative Disease

Diffusion tensor imaging has also been used to evaluate patients with neurodegenerative diseases. White matter starts to undergo changes with age at a microstructural level, including neuronal shrinkage, demyelination and axonal changes that are demonstrated as hyperintensities on T2-weighted MR imaging (45). DTI studies in aging patients have revealed that reduced FA and increased MD in the frontal white matter (WM) and the genu of the corpus callosum may result in cognitive decline (46, 47). On the other hand, in patients with Alzheimer's disease, DTI has shown reduced anisotropy in the parietal and temporal WM, the corpus callosum and the posterior cingulum fibers (and the latter connects the parahippocampal gyrus and posterior cingulated gyrus) due to neurodegenerative processes (48). Similarly, patients with Alzheimer's disease or frontotemporal lobar degeneration have shown decreased

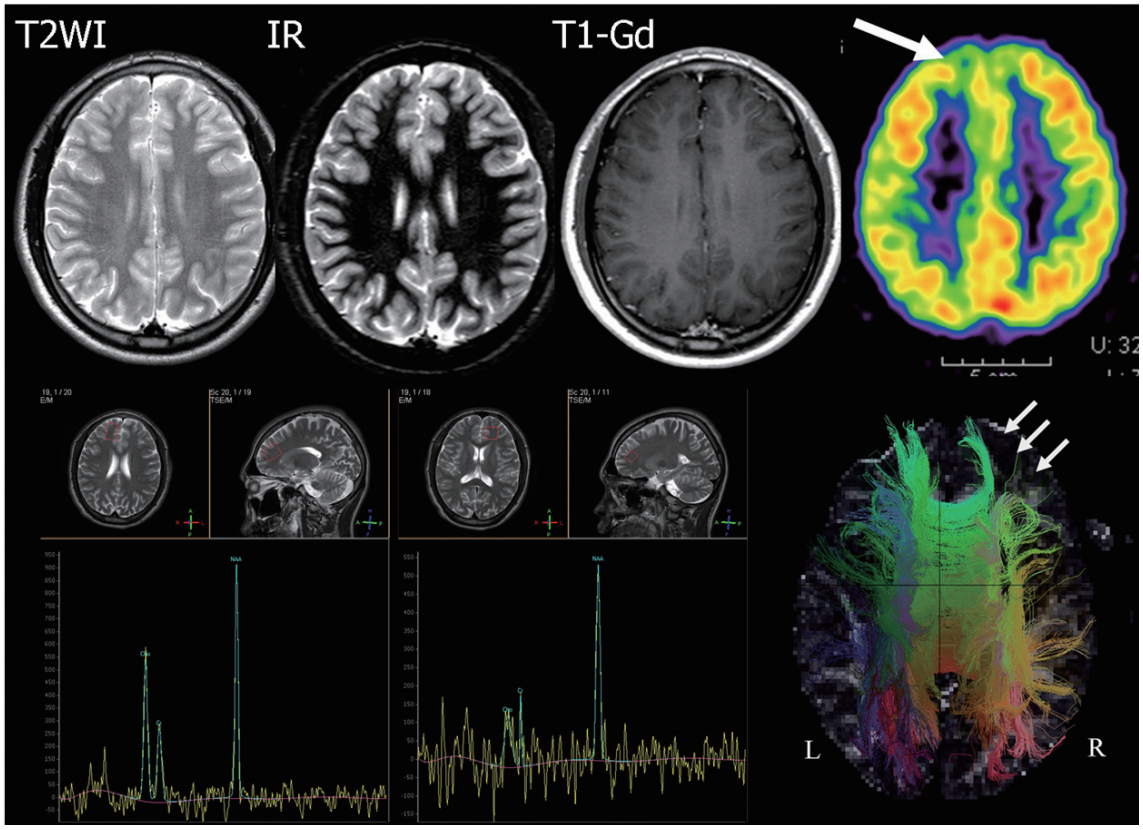

Fig. 12. 8-year-old male with intractable seizure. Conventional spin-echo and inversion recovery (IR) MRI shows no definite abnormality of frontal cortex. PET demonstrates decreased metabolism at right frontal cortex (thick arrow). MR spectroscopy describes increased choline level in right frontal cortex. Tractography of both hemispheres reveals decreased subcortical fiber connectivity in left frontal cortex (thin arrows). In this case, tractography was more sensitive than other conventional MRI modalities and it can be compared with PET or MR spectroscopy.

FA and increased MD in the bilateral uncinate fasciculus, which is believed to play a role in cognitive and memory function, and the values of diffusivity were subsequently correlated with the severity of the disease process (49, 50). In addition, reduced anisotropy in the posterior cingulum, temporal WM, parietal WM and parahippocampal WM was found in mild cognitive impairment and a continuum spanning from normal aging to Alzheimer's disease, with greater posterior than anterior involvement (7, 48). It was reported that 11-17% of individuals with mild cognitive impairment progress to dementia annually (51), and so DTI may be useful for the early identification of patients with mild cognitive impairment and who are at risk of progressing to dementia.

A previous study using DTI reported that de novo patients with Parkinson disease can be distinguished from healthy individuals even in the early stage with high accuracy by demonstrating reduced FA in the substantial nigra and especially in the caudal segment (52). These results suggested that DTI has the potential to serve as a noninvasive early biomarker for Parkinson disease.

Psychiatric Disease

Diffusion tensor imaging has been used for demonstrating WM abnormalities as quantified by anisotropy measures in a variety of psychiatric diseases such as schizophrenia, behavior disorder and mood disorder (8, 53). Among them, schizophrenia is one of the most commonly investigated psychiatric diseases. Although the findings in schizophrenia are inconsistent across DTI studies in terms of the affected brain regions, including the corpus callosum, the arcuate fasciculus, the cingulum bundle and the cerebellar peduncles, many studies have identified reduced FA in the frontal and temporal WM and this suggested that a disturbance in connectivity between different brain areas may be responsible for the clinical symptoms (53-55).

Limitations

Diffusion tensor imaging and FT provide useful anatomic information and they can be applied to many maladies/clinical settings, but of course there are limitations.

First, although there have been attempts to validate these imaging techniques histologically and radiologically,

Korean Journal of Radiology
KJR

there is no gold standard for *in vivo* FT (56-58).

Second, as DTI provides indirect information about axonal structures by averaging the water diffusion properties within a voxel (10), and many pathways can be obscured by the dominant nerve fibers or the fiber trajectories may fail to follow crossed or branching fibers, or even phantom connections are depicted. If there is a nonuniform distribution of fiber directions, then the eigenvector associated with the largest eigenvalue only corresponds to the averaged fiber direction within the voxel, and this may not necessarily reflex the nerve fibers crossing the voxel. This shortcoming of FT based on the diffusion tensor model could be mitigated with high-angular resolution diffusion imaging such as q-ball imaging, a multitensor model and diffusion spectral imaging by sampling more diffusion weighted directions with stronger diffusion gradients (59).

Third, many factors may influence the ability of DTI in clinical applications. The fiber tracking technique is highly operator-dependent. Therefore, the standard ROI location and placement of an adequate threshold value for fiber tracking are essential for achieving an objective, uniform fiber tracking result. Further, the field strength of the magnet and the spatial resolution may affect the image quality of DTI. Additionally, noise and artifacts such as eddy currents, and susceptibility and motion artifacts result in uncertainty about the orientation of the diffusion tensor and the position of fiber tracks.

CONCLUSION

As DTI and FT become more widely used for diagnosis and treatment, it is critical for radiologists to understand the capabilities and limitations of these techniques. Future improvements of the MR hardware and imaging techniques will allow routinely performing tractography in the clinical setting. Yet this technique needs to be standardized to obtain objective and reproducible results.

REFERENCES

1. Le Bihan D, Breton E, Lallemand D, Grenier P, Cabanis E, Laval-Jeantet M. MR imaging of intravoxel incoherent motions: application to diffusion and perfusion in neurologic disorders. *Radiology* 1986;161:401-407
2. Mori S, Oishi K, Faria AV. White matter atlases based on diffusion tensor imaging. *Curr Opin Neurol* 2009;22:362-369
3. Berman J. Diffusion MR tractography as a tool for surgical planning. *Magn Reson Imaging Clin N Am* 2009;17:205-214
4. Pizzini FB, Polonara G, Mascioli G, Beltramello A, Foroni R, Paggi A, et al. Diffusion tensor tracking of callosal fibers several years after callosotomy. *Brain Res* 2010;1312:10-17
5. Yang Q, Tress BM, Barber PA, Desmond PM, Darby DG, Gerraty RP, et al. Serial study of apparent diffusion coefficient and anisotropy in patients with acute stroke. *Stroke* 1999;30:2382-2390
6. Lee SK, Kim DI, Kim J, Kim DJ, Kim HD, Kim DS, et al. Diffusion-tensor MR imaging and fiber tractography: a new method of describing aberrant fiber connections in developmental CNS anomalies. *Radiographics* 2005;25:53-65; discussion 66-58
7. Zhang Y, Schuff N, Jahng GH, Bayne W, Mori S, Schad L, et al. Diffusion tensor imaging of cingulum fibers in mild cognitive impairment and Alzheimer disease. *Neurology* 2007;68:13-19
8. Kubicki M, Westin CF, Maier SE, Mamata H, Frumin M, Ersner-Hershfield H, et al. Diffusion tensor imaging and its application to neuropsychiatric disorders. *Harv Rev Psychiatry* 2002;10:324-336
9. Chenevert TL, Brunberg JA, Pipe JG. Anisotropic diffusion in human white matter: demonstration with MR techniques in vivo. *Radiology* 1990;177:401-405
10. Pierpaoli C, Jezzard P, Basser PJ, Barnett A, Di Chiro G. Diffusion tensor MR imaging of the human brain. *Radiology* 1996;201:637-648
11. Jones DK, Horsfield MA, Simmons A. Optimal strategies for measuring diffusion in anisotropic systems by magnetic resonance imaging. *Magn Reson Med* 1999;42:515-525
12. Papadakis NG, Xing D, Huang CL, Hall LD, Carpenter TA. A comparative study of acquisition schemes for diffusion tensor imaging using MRI. *J Magn Reson* 1999;137:67-82
13. Hasan KM, Parker DL, Alexander AL. Comparison of gradient encoding schemes for diffusion-tensor MRI. *J Magn Reson Imaging* 2001;13:769-780
14. Jones DK. The effect of gradient sampling schemes on measures derived from diffusion tensor MRI: a Monte Carlo study. *Magn Reson Med* 2004;51:807-815
15. Turner R, Le Bihan D, Chesnick AS. Echo-planar imaging of diffusion and perfusion. *Magn Reson Med* 1991;19:247-253
16. Anderson AW, Gore JC. Analysis and correction of motion artifacts in diffusion weighted imaging. *Magn Reson Med* 1994;32:379-387
17. Ordidge RJ, Helpern JA, Qing ZX, Knight RA, Nagesh V. Correction of motional artifacts in diffusion-weighted MR images using navigator echoes. *Magn Reson Imaging* 1994;12:455-460
18. Papadakis NG, Martin KM, Mustafa MH, Wilkinson ID, Griffiths PD, Huang CL, et al. Study of the effect of CSF suppression on white matter diffusion anisotropy mapping of healthy human brain. *Magn Reson Med* 2002;48:394-398
19. Yamada K, Kizu O, Mori S, Ito H, Nakamura H, Yuen S, et al. Brain fiber tracking with clinically feasible diffusion-tensor MR imaging: initial experience. *Radiology* 2003;227:295-301
20. Okada T, Miki Y, Fushimi Y, Hanakawa T, Kanagaki M, Yamamoto A, et al. Diffusion-tensor fiber tractography:

intraindividual comparison of 3.0-T and 1.5-T MR imaging. *Radiology* 2006;238:668-678
21. Nagae-Poetscher LM, Jiang H, Wakana S, Golay X, van Zijl PC, Mori S. High-resolution diffusion tensor imaging of the brain stem at 3 T. *AJNR Am J Neuroradiol* 2004;25:1325-1330
22. Le Bihan D, Mangin JF, Poupon C, Clark CA, Pappata S, Molko N, et al. Diffusion tensor imaging: concepts and applications. *J Magn Reson Imaging* 2001;13:534-546
23. Douek P, Turner R, Pekar J, Patronas N, Le Bihan D. MR color mapping of myelin fiber orientation. *J Comput Assist Tomogr* 1991;15:923-929
24. Mori S, Crain BJ, Chacko VP, van Zijl PC. Three-dimensional tracking of axonal projections in the brain by magnetic resonance imaging. *Ann Neurol* 1999;45:265-269
25. Behrens TE, Woolrich MW, Jenkinson M, Johansen-Berg H, Nunes RG, Clare S, et al. Characterization and propagation of uncertainty in diffusion-weighted MR imaging. *Magn Reson Med* 2003;50:1077-1088
26. Behrens TE, Berg HJ, Jbabdi S, Rushworth MF, Woolrich MW. Probabilistic diffusion tractography with multiple fibre orientations: What can we gain? *Neuroimage* 2007;34:144-155
27. Oishi K, Zilles K, Amunts K, Faria A, Jiang H, Li X, et al. Human brain white matter atlas: identification and assignment of common anatomical structures in superficial white matter. *Neuroimage* 2008;43:447-457
28. Lee JS, Han MK, Kim SH, Kwon OK, Kim JH. Fiber tracking by diffusion tensor imaging in corticospinal tract stroke: Topographical correlation with clinical symptoms. *Neuroimage* 2005;26:771-776
29. Geyer S, Matelli M, Luppino G, Zilles K. Functional neuroanatomy of the primate isocortical motor system. *Anat Embryol (Berl)* 2000;202:443-474
30. Guye M, Parker GJ, Symms M, Boulby P, Wheeler-Kingshott CA, Salek-Haddadi A, et al. Combined functional MRI and tractography to demonstrate the connectivity of the human primary motor cortex in vivo. *Neuroimage* 2003;19:1349-1360
31. Laundre BJ, Jellison BJ, Badie B, Alexander AL, Field AS. Diffusion tensor imaging of the corticospinal tract before and after mass resection as correlated with clinical motor findings: preliminary data. *AJNR Am J Neuroradiol* 2005;26:791-796
32. Lazar M, Alexander AL, Thottakara PJ, Badie B, Field AS. White matter reorganization after surgical resection of brain tumors and vascular malformations. *AJNR Am J Neuroradiol* 2006;27:1258-1271
33. Lu S, Ahn D, Johnson G, Cha S. Peritumoral diffusion tensor imaging of high-grade gliomas and metastatic brain tumors. *AJNR Am J Neuroradiol* 2003;24:937-941
34. Lu S, Ahn D, Johnson G, Law M, Zagzag D, Grossman RI. Diffusion-tensor MR imaging of intracranial neoplasia and associated peritumoral edema: introduction of the tumor infiltration index. *Radiology* 2004;232:221-228
35. Powell HW, Parker GJ, Alexander DC, Symms MR, Boulby PA, Wheeler-Kingshott CA, et al. MR tractography predicts visual field defects following temporal lobe resection. *Neurology* 2005;65:596-599
36. Jea A, Vachhrajani S, Widjaja E, Nilsson D, Raybaud C, Shroff M, et al. Corpus callosotomy in children and the disconnection syndromes: a review. *Childs Nerv Syst* 2008;24:685-692
37. Klatzo I. Pathophysiological aspects of brain edema. *Acta Neuropathol* 1987;72:236-239
38. Davis D, Ulatowski J, Eleff S, Izuta M, Mori S, Shungu D, et al. Rapid monitoring of changes in water diffusion coefficients during reversible ischemia in cat and rat brain. *Magn Reson Med* 1994;31:454-460
39. Carano RA, Li F, Irie K, Helmer KG, Silva MD, Fisher M, et al. Multispectral analysis of the temporal evolution of cerebral ischemia in the rat brain. *J Magn Reson Imaging* 2000;12:842-858
40. Nelles M, Gieseke J, Flacke S, Lachenmayer L, Schild HH, Urbach H. Diffusion tensor pyramidal tractography in patients with anterior choroidal artery infarcts. *AJNR Am J Neuroradiol* 2008;29:488-493
41. Hosomi A, Nagakane Y, Yamada K, Kuriyama N, Mizuno T, Nishimura T, et al. Assessment of arcuate fasciculus with diffusion-tensor tractography may predict the prognosis of aphasia in patients with left middle cerebral artery infarcts. *Neuroradiology* 2009;51:549-555
42. McKinstry RC, Mathur A, Miller JH, Ozcan A, Snyder AZ, Schefft GL, et al. Radial organization of developing preterm human cerebral cortex revealed by non-invasive water diffusion anisotropy MRI. *Cereb Cortex* 2002;12:1237-1243
43. Eriksson SH, Symms MR, Rugg-Gunn FJ, Boulby PA, Wheeler-Kingshott CA, Barker GJ, et al. Exploring white matter tracts in band heterotopia using diffusion tractography. *Ann Neurol* 2002;52:327-334
44. Hoon AH Jr, Lawrie WT Jr, Melhem ER, Reinhardt EM, Van Zijl PC, Solaiyappan M, et al. Diffusion tensor imaging of periventricular leukomalacia shows affected sensory cortex white matter pathways. *Neurology* 2002;59:752-756
45. Kapeller P, Schmidt R, Fazekas F. Qualitative MRI: evidence of usual aging in the brain. *Top Magn Reson Imaging* 2004;15:343-347
46. Salat DH, Tuch DS, Greve DN, van der Kouwe AJ, Hevelone ND, Zaleta AK, et al. Age-related alterations in white matter microstructure measured by diffusion tensor imaging. *Neurobiol Aging* 2005;26:1215-1227
47. Charlton RA, Barrick TR, McIntyre DJ, Shen Y, O'Sullivan M, Howe FA, et al. White matter damage on diffusion tensor imaging correlates with age-related cognitive decline. *Neurology* 2006;66:217-222
48. Medina D, DeToledo-Morrell L, Urresta F, Gabrieli JD, Moseley M, Fleischman D, et al. White matter changes in mild cognitive impairment and AD: A diffusion tensor imaging study. *Neurobiol Aging* 2006;27:663-672
49. Taoka T, Iwasaki S, Sakamoto M, Nakagawa H, Fukusumi A, Myochin K, et al. Diffusion anisotropy and diffusivity of white matter tracts within the temporal stem in Alzheimer disease: evaluation of the "tract of interest" by diffusion tensor tractography. *AJNR Am J Neuroradiol* 2006;27:1040-1045

50. Matsuo K, Mizuno T, Yamada K, Akazawa K, Kasai T, Kondo M, et al. Cerebral white matter damage in frontotemporal dementia assessed by diffusion tensor tractography. *Neuroradiology* 2008;50:605-611
51. Ganguli M, Dodge HH, Shen C, DeKosky ST. Mild cognitive impairment, amnestic type: an epidemiologic study. *Neurology* 2004;63:115-121
52. Vaillancourt DE, Spraker MB, Prodoehl J, Abraham I, Corcos DM, Zhou XJ, et al. High-resolution diffusion tensor imaging in the substantia nigra of de novo Parkinson disease. *Neurology* 2009;72:1378-1384
53. Kubicki M, McCarley R, Westin CF, Park HJ, Maier S, Kikinis R, et al. A review of diffusion tensor imaging studies in schizophrenia. *J Psychiatr Res* 2007;41:15-30
54. Kyriakopoulos M, Bargiotas T, Barker GJ, Frangou S. Diffusion tensor imaging in schizophrenia. *Eur Psychiatry* 2008;23:255-273
55. Kanaan RA, Kim JS, Kaufmann WE, Pearlson GD, Barker GJ, McGuire PK. Diffusion tensor imaging in schizophrenia. *Biol Psychiatry* 2005;58:921-929
56. Scollan DF, Holmes A, Winslow R, Forder J. Histological validation of myocardial microstructure obtained from diffusion tensor magnetic resonance imaging. *Am J Physiol* 1998;275:H2308-2318
57. Lin CP, Tseng WY, Cheng HC, Chen JH. Validation of diffusion tensor magnetic resonance axonal fiber imaging with registered manganese-enhanced optic tracts. *Neuroimage* 2001;14:1035-1047
58. Okada T, Mikuni N, Miki Y, Kikuta K, Urayama S, Hanakawa T, et al. Corticospinal tract localization: integration of diffusion-tensor tractography at 3-T MR imaging with intraoperative white matter stimulation mapping--preliminary results. *Radiology* 2006;240:849-857
59. Hagmann P, Jonasson L, Maeder P, Thiran JP, Wedeen VJ, Meuli R. Understanding diffusion MR imaging techniques: from scalar diffusion-weighted imaging to diffusion tensor imaging and beyond. *Radiographics* 2006;26 Suppl 1:S205-223